

See discussions, stats, and author profiles for this publication at: <https://www.researchgate.net/publication/260607026>

Target Turing Patterns and Growth Dynamics in the Chlorine Dioxide-Iodine-Malonic Acid Reaction

ARTICLE in THE JOURNAL OF PHYSICAL CHEMISTRY A · MARCH 2014

Impact Factor: 2.69 · DOI: 10.1021/jp500432t · Source: PubMed

CITATIONS

4

READS

57

3 AUTHORS:



Asher Preska Steinberg
California Institute of Technology

5 PUBLICATIONS 193 CITATIONS

[SEE PROFILE](#)



Irving R Epstein
Brandeis University
412 PUBLICATIONS 11,591 CITATIONS

[SEE PROFILE](#)



Milos Dolnik
Brandeis University
65 PUBLICATIONS 2,272 CITATIONS

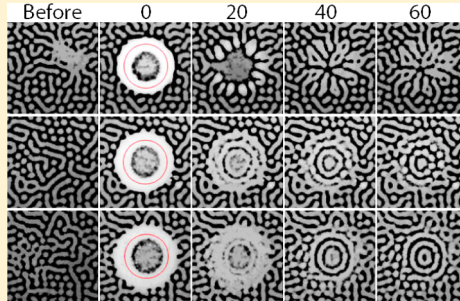
[SEE PROFILE](#)

Target Turing Patterns and Growth Dynamics in the Chlorine Dioxide–Iodine–Malonic Acid Reaction

Asher Preska Steinberg[†], Irving R. Epstein, and Milos Dolnik*

Department of Chemistry, Brandeis University, Waltham, Massachusetts 02454-9110, United States

ABSTRACT: We study the growth dynamics of Turing patterns in the chlorine dioxide–iodine–malonic acid reaction–diffusion system in response to perturbations with visible light. We describe several mechanisms by which Turing patterns reappear after they are suppressed by illumination with a disc-shaped geometry. We observe that under specific conditions the patterns reorganize from a random configuration of spots and stripes to a set of ordered, concentric rings, which we refer to as target Turing patterns. These patterns closely resemble the unit cells of the Turing hexagonal superlattices known as black eye patterns. However, these target Turing patterns are not part of a larger superlattice structure, and they usually have a larger number of concentric rings. Numerical simulations support the experimental findings.



INTRODUCTION

In 1952 Alan Turing suggested that, under appropriate conditions, spatially periodic, stationary patterns could form in nonequilibrium reaction–diffusion systems.¹ These patterns are now known as Turing patterns (TP). Turing's theory offered a plausible mechanism for morphogenesis. His theory provides a possible explanation for structures throughout biology, including the patterns on the coats of leopards, giraffes and zebras,² and the skin of tropical fish.^{3,4} It has even been proposed that the morphogenesis of labyrinthine patterns in the human brain may be an example of TP formation.⁵ TP have also been found in other fields; stripe TP have been observed in gas discharge semiconductor systems⁶ and in the growth of semiconductor nanostructures.⁷ Ecologists have shown that certain reaction–diffusion predator–prey models can give rise to TP in the distribution of animals.⁸

Almost 40 years after Turing's theoretical work, the first experimental evidence of TP was established using the chlorite–iodide–malonic acid (CIMA) reaction.⁹ This discovery triggered renewed interest in TP, and since then much effort has been put into experimental studies of TP.^{10,11} There has also been strong interest in applying perturbations of different symmetries to chemical systems to manipulate pattern formation.¹² It has been shown that visible light can be used to control and manipulate TP in the photosensitive chlorine dioxide–iodine–malonic acid (CDIMA) reaction.¹³ In this reaction, which is a modified version of the CIMA reaction, molecular iodine photodissociates in the presence of white light, and the iodine atoms react quickly with other species in the CDIMA reaction, reducing chlorine dioxide and oxidizing iodide ions.¹⁴ In the areas exposed to light the patterns lose their dark color because the concentration of iodide is depleted, which lowers the concentration of the dark triiodide complex with starch or polyvinyl alcohol. Chlorine dioxide also plays a significant role in the photosensitivity of the CDIMA reaction.¹⁵

The photosensitivity of the CDIMA reaction–diffusion system makes it an excellent medium in which to produce TP with unique geometries. Illumination patterns with wavelengths that are specific multiples of the intrinsic wavelength of the TP have been used to induce hexagonal and square pattern superlattices in the CDIMA reaction–diffusion system.^{16–18} Wavenumber-locking of TP under stripe^{19,20} and square²¹ forcing has also been investigated. Most of these studies focus on the different types of stationary TP; somewhat less attention has been devoted to the growth dynamics of TP.

Davies et al.²² examined the growth dynamics of TP in the CDIMA reaction–diffusion system after a sudden change in one of the feeding reagent concentrations. This change was designed to shift the system from a steady state to a TP domain. A small silver particle was placed inside the reactor to control the location at which pattern formation was nucleated. The patterns initiated at the nucleation point grew outward and produced “flower-like” patterns or “dividing blobs”. In another study, Míguez et al.²³ investigated the formation of TP in a system that allows for continuous growth in one direction. Depending on the growth velocity, they obtained three different configurations of TP: stripes that are parallel, oblique, or perpendicular to the growth direction.

It has been demonstrated that novel and unique spatial temporal patterns can be induced, modified, and guided in reaction diffusion systems by local perturbation^{24,25} or by a feedback mechanism.²⁶ In this work we apply a similar technique to Turing patterns, and we demonstrate that some patterns that are unlikely to form spontaneously can be induced by local perturbation. We study the growth dynamics of Turing patterns in the CDIMA reaction–diffusion system in response

Received: January 14, 2014

Revised: March 5, 2014

Published: March 6, 2014

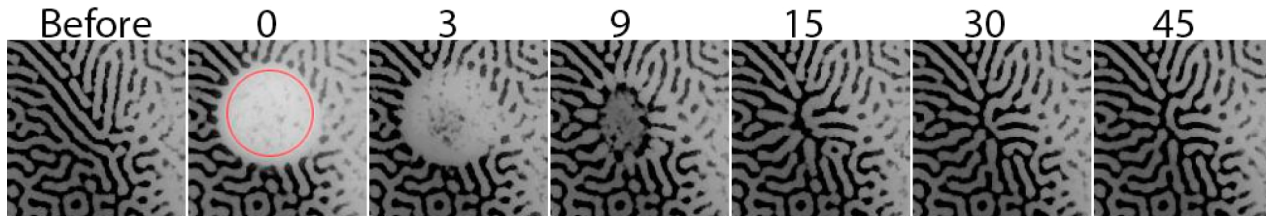


Figure 1. Regrowth of TP by fingering mechanism after disc-shaped perturbation (diameter, $D = 2.7$ mm). The size of perturbation is indicated by the red circle in the second column. Each frame is 5.15×5.15 mm. The first column shows patterns right before the perturbation, the second column is immediately after, and remaining columns are then up to 45 min after (numbers above figures are in minutes). $[MA] = 1$ mM and $[ClO_2] = 0.2$ mM. The intensity of the disc-shaped illumination is $I_{disc} = 57.3$ mW cm $^{-2}$.

to perturbations with visible light. In particular, we describe different mechanisms by which TP reappear after they are suppressed by illumination with a disc-shaped geometry. Our studies of the growth dynamics of TP reveal a uniquely shaped stripe TP. We observe that under certain conditions the pattern reorganizes after a disc-shaped perturbation from a random configuration of spots and stripes to a set of ordered, concentric rings, which we refer to as target TP. The appearance of these patterns strongly resembles a snapshot of target patterns of propagating wave fronts.²⁷ However, these patterns do not propagate; they are stationary in time. The target TP also closely resemble the unit cells of the Turing hexagonal superlattices known as black eye patterns.^{12–14,28} The key differences are that target TP are not part of a larger superlattice structure, and target TP can contain a greater number of concentric rings, not just one or two. We investigate the different conditions under which target TP can develop in the CDIMA reaction-diffusion system, what factors allow them to form, and what sizes of target TP can form.

■ EXPERIMENTAL METHODS

Experimental Setup. The reaction was carried out in a continuously fed unstirred reactor (CFUR) placed on top of a continuously fed stirred tank reactor (CSTR).^{20,21} The volume of the CSTR compartment was 2.7 mL, and the reaction mixture in the CSTR was homogenized by three magnetic stir bars that rotated at a constant speed of 1000 rpm. Pattern formation took place in the CFUR, which was a 2% agarose gel (Acros, thickness 0.3 mm, diameter 25 mm). The reagents were continuously fed into the CSTR compartment. An Anopore and a cellulose nitrate membrane were placed between the CSTR and CFUR compartments. The Anopore membrane (Whatman, pore size 0.2 μ m, impregnated with 4% agarose gel, total thickness of 0.10 mm) separated the CFUR from the vigorous stirring in the CSTR and gave stiff support to the gel. The cellulose nitrate membrane (Whatman, pore size 0.45 μ m, thickness 0.12 mm) was placed underneath the gel to increase the contrast of the patterns. Above the CFUR was an impermeable optical glass window through which the system was illuminated. The reactor was placed in a thermostatic bath to keep the temperature constant at 4.0 ± 0.2 °C.

Grayscale images were projected onto the system using a projector (Dell 1510X) and a beam splitter (Edmund Optics). A planoconvex lens was used to focus the projected light on the surface of the reactor. Images were taken with a CCD camera (Pixelink, PL-B956), which was controlled by a PC. To visualize the patterns, the system was illuminated with ambient light ($I = 1.2$ mW cm $^{-2}$) using a 30 W quartz halogen lamp (Dolan-Jenner, Fiber-Lite Model 190). MATLAB software was used to calculate 2D Fast Fourier Transforms to evaluate the

wavelength of the patterns and to produce images used for the system illumination.

Materials. Three reagent solutions were fed into the CSTR by peristaltic pumps (Rainin): (i) a mixture of malonic acid (MA, Aldrich) and poly(vinyl alcohol) (PVA, Aldrich, average molecular weight 9000–10000); (ii) I_2 (Aldrich, 99.8%); (iii) ClO_2 prepared as described in ref 29. The iodine solution contained 10% by volume CH_3COOH (Fisher Scientific) to help dissolve the iodine in the preparation of the solution and to prevent it from precipitating out when it was fed into the CSTR. PVA acts as a color indicator and binds triiodide ions. It slows the diffusion of iodide in solution, which is necessary for Turing pattern formation. The following parameters were fixed and kept the same in all experiments: $[I_2] = 0.4$ mM, $[PVA] = 10$ g/L, $[H_2SO_4] = 10$ mM. The residence time of the reactants in the CSTR was 130 s.

■ EXPERIMENTAL RESULTS

After the reaction was started in our setup, it took several hours for TP to spontaneously develop and become stationary. When the pattern became stationary, disc-shaped strong illumination ($I_{disc} = 57.3$ mW cm $^{-2}$) was applied to a selected area. Snapshots of patterns were taken right before the perturbation, immediately after, and then every 1–2 min up to 45–180 min after the initial perturbation.

To investigate the growth dynamics of TP, we monitored the system responses to illumination when different concentrations of ClO_2 and MA were used. In these experiments the illumination was applied for 2 min and the system was allowed to recover for 45 min or more. The concentration of ClO_2 was varied between 0.07 and 0.20 mM and that of MA between 0.5 and 3.0 mM. Selected results of these experiments are shown in Figures 1–3. Immediately after the perturbation was applied, the patterns were suppressed in the illuminated area. This area appears much brighter, because the concentration of the PVA–triiodide complex in the region decreases due to the depletion of iodide ions. Generally, within the first 10 min after illumination, the perturbed area began to darken as the iodide and PVA–triiodide concentrations in this area started to increase.

One type of growth mechanism that we observed was a “fingering” mechanism (Figure 1). The patterns elongated at the edges of the perturbed regions, and finger-like patterns spread out and started to fill the space. A similar mechanism was observed by Davies et al. in the formation of “chemical flowers”.²² There is a difference, though; here the patterns grow inward from the perimeter of the perturbed region toward the center, as opposed to the “chemical flowers”, which grow outward from a center.

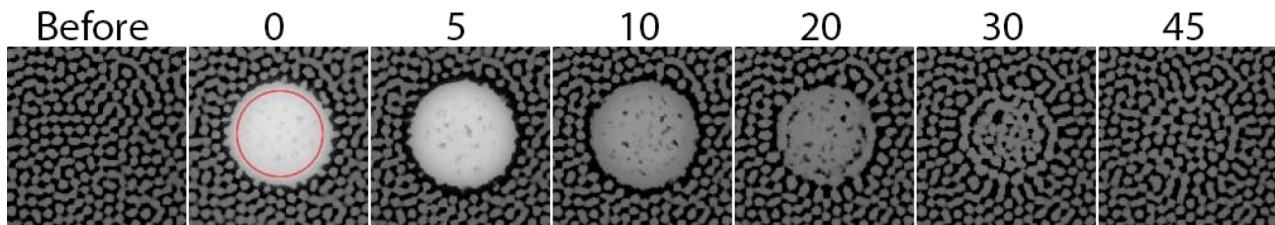


Figure 2. Random growth of TP in response to disc-shaped perturbations ($D = 2.7$ mm, $I_{\text{disc}} = 57.3$ mW cm $^{-2}$). The size of perturbation is indicated by the red circle in the second column. Each frame is 5.15×5.15 mm. The first column shows patterns right before perturbation, the second column is immediately after, and remaining columns are then up to 45 min after (numbers above figures are in minutes). $[\text{MA}] = 0.7$ mM and $[\text{ClO}_2] = 0.2$ mM.

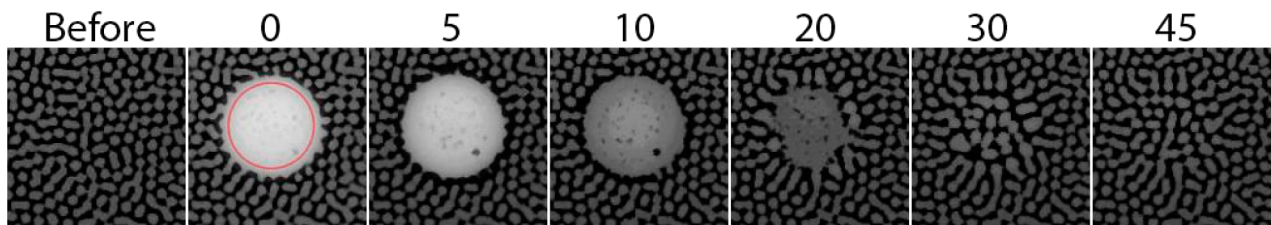


Figure 3. Regrowth of TP in response to disc-shaped perturbations ($D = 2.7$ mm, $I_{\text{disc}} = 57.3$ mW cm $^{-2}$) by both the fingering mechanism and random growth. The size of perturbation is indicated by the red circle in the second column. Each frame is 5.15×5.15 mm. The first column shows patterns right before perturbation, the second column is immediately after, and remaining columns are then up to 45 min after (numbers above figures are in minutes). $[\text{MA}] = 0.7$ mM and $[\text{ClO}_2] = 0.1$ mM.

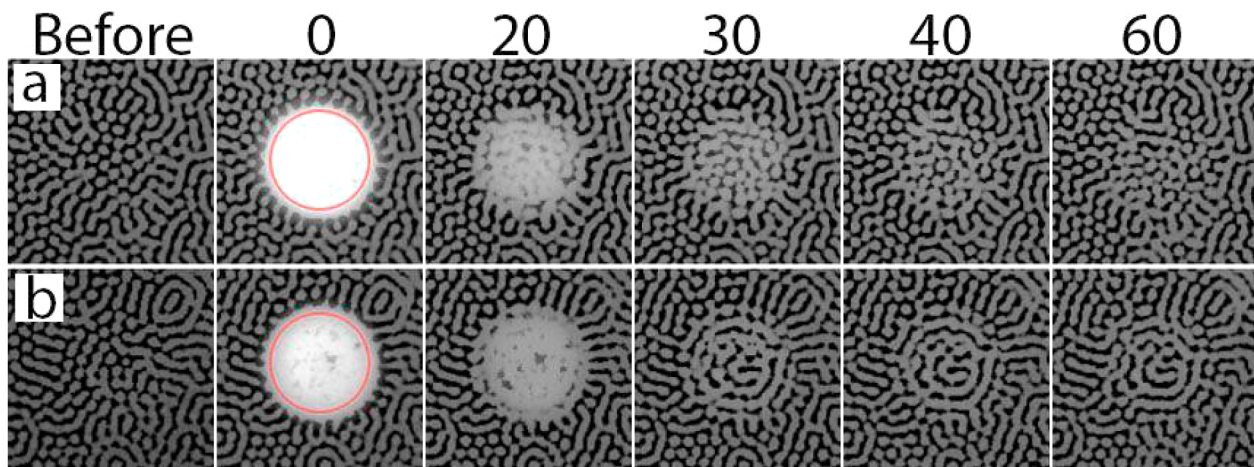


Figure 4. Response of the system to disc-shaped perturbations ($D = 2.7$ mm, $I_{\text{disc}} = 57.3$ mW cm $^{-2}$) with different intensities of background illumination. Background illumination: $I =$ (a) 2.1 and (b) 3.0 mW cm $^{-2}$. The size of the perturbation is indicated by the red circle in the second column. Each frame is 5.15×5.15 mm. The first column shows the patterns just before the perturbation, the second column is immediately after, and remaining columns are then up to 60 min after (numbers above figures are in minutes). For all rows $[\text{MA}] = 1$ mM and $[\text{ClO}_2] = 0.2$ mM.

We also observed the growth of patterns from random points in the perturbed area (Figure 2). We refer to this mechanism as “random growth”. In most cases, the patterns grew back through a combination of both mechanisms. Fingers began to grow from the edges of the perturbed region, followed by the center of the space being filled by patterns resulting from random growth, as shown in Figure 3.

We noticed that exposure to ambient light of increased intensity from the 30 W quartz halogen lamp used to visualize the patterns affected the system regrowth dynamics. Therefore, we further examined the effect of background illumination intensity on the regrowth dynamics of TP by allowing the suppressed areas to recover under weak illumination (Figure 4). The intensity of the background illumination ranged from $I = 1.2$ to $I = 5.4$ mW cm $^{-2}$ (values of intensity given include that

of the light from the projector and the ambient light source). When the intensity of the background illumination was below $I = 2.1$ mW cm $^{-2}$, we did not observe any obvious effects on the final pattern after the perturbation or on the regrowth dynamics of TP. When the intensity of the background illumination reached or exceeded about 3 mW cm $^{-2}$, we observed that the final pattern had a different spatial arrangement compared to the original pattern. Figure 4a shows snapshots of TP that consist of mixtures of stripes and spots under weak intensity background illumination ($I = 2.1$ mW cm $^{-2}$). Both before and after the perturbation the TP remained as mostly spots with a few stripes. In Figure 4b with stronger background illumination ($I = 3.0$ mW cm $^{-2}$), the spatial arrangement of the pattern 1 h after the perturbation was visually different from the original pattern and consisted of mostly stripes and just a few spots.

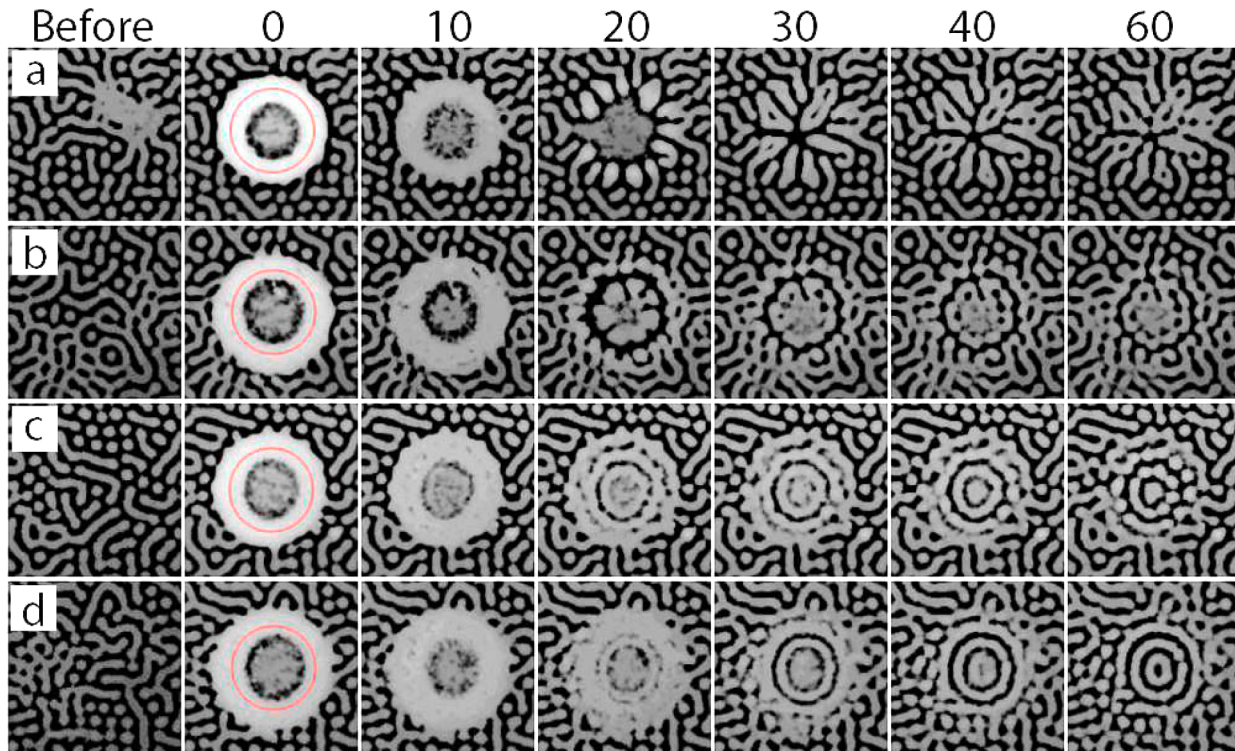


Figure 5. Regrowth of TP after suppression as a function of background illumination intensity. The patterns recovered in light with an intensity of $I =$ (a) 1.2, (b) 3.0, (c) 4.6, and (d) 5.4 mW cm^{-2} . The strong disc-shaped illumination ($D = 2.7 \text{ mm}$, $I_{\text{disc}} = 57.3 \text{ mW cm}^{-2}$, indicated by the red circles in the second column) was applied for 10 min. Each frame is $5.15 \times 5.15 \text{ mm}$. The first column shows patterns right before the perturbation, the second right after, and remaining columns are then up to 60 min after (numbers above figures are in minutes). For all rows, $[\text{ClO}_2] = 0.07 \text{ mM}$ and $[\text{MA}] = 1 \text{ mM}$.

Even when the final pattern had a different appearance than the pattern before the perturbation, the initial and final wavelengths were not significantly different (the largest observed difference was 0.04 mm, which is about 10% of the pattern wavelength).

When the strong disc-shaped illumination was applied for a longer period of time and the system was allowed to recover in background illumination of sufficiently high intensity, we observed the formation of a stripe pattern that formed in an ordered structure of concentric rings, which we refer to as target TP (Figure 5). When pattern recovery took place under low intensity background illumination ($I = 1.2 \text{ mW cm}^{-2}$), a typical labyrinthine TP was produced from the edges of the suppressed area via the fingering mechanism, and no target TP were obtained. In Figure 5b with background illumination of $I = 3.0 \text{ mW cm}^{-2}$, patterns formed as fingers moving inward from the edges of the perturbed area, while at the same time patterns grew outward from the center, similar to the chemical flowers observed by Davies et al.²² With stronger background illumination (Figure 5c,d), target TP formed from the center of the suppressed area. We conclude that the intensity of the background illumination has an effect on whether or not patterns form from the edges or center of the perturbed area, and that higher intensity background illumination supports the formation of target TP.

The duration of the strong disc-shaped illumination affected whether or not the patterns reorganized into target TP. Figure 6 shows two different experiments we carried out in which discs of light were applied for 2 and 10 min. Target TP failed to develop if the illumination was applied for only 2 min. The patterns only reorganized into target TP with illumination that lasted for 10 min or more. We also noticed that with longer

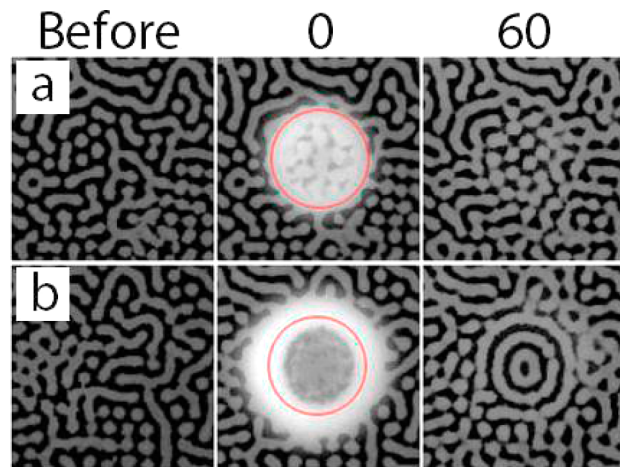


Figure 6. Effect of duration of illumination on the growth of TP. The disc-shaped illumination ($D = 2.7 \text{ mm}$, $I_{\text{disc}} = 57.3 \text{ mW cm}^{-2}$) in (a) is applied for 2 min and (b) 10 min. The size of the perturbation is indicated by the red circles in the second column. Each frame is $5.15 \times 5.15 \text{ mm}$. The first column shows patterns right before perturbation, the second right after, and the third is 60 min after (numbers above figures are in minutes). For all rows, $[\text{ClO}_2] = 0.07 \text{ mM}$ and $[\text{MA}] = 1 \text{ mM}$. The intensity of the background illumination is $I = 5.4 \text{ mW cm}^{-2}$.

illumination a dark spot would form in the center of the perturbed area (Figure 6b). It appears that the dark spot that forms after suppression of patterns using strong illumination plays an important role in the formation of target TP.

To better understand how the dark spot forms in the center, we applied strong disc-shaped illumination for 10 min and

observed how the illuminated pattern and suppressed area changed during the illumination. Several experiments were carried out with different concentrations of ClO_2 : $[\text{ClO}_2] = 0.05, 0.07, 0.10, 0.14, 0.20 \text{ mM}$. For $[\text{ClO}_2] = 0.10\text{--}0.20 \text{ mM}$, we observed that as we increased the time for which the perturbation was applied, the region where the patterns were suppressed became larger (Figure 7a,b). After 5 min of

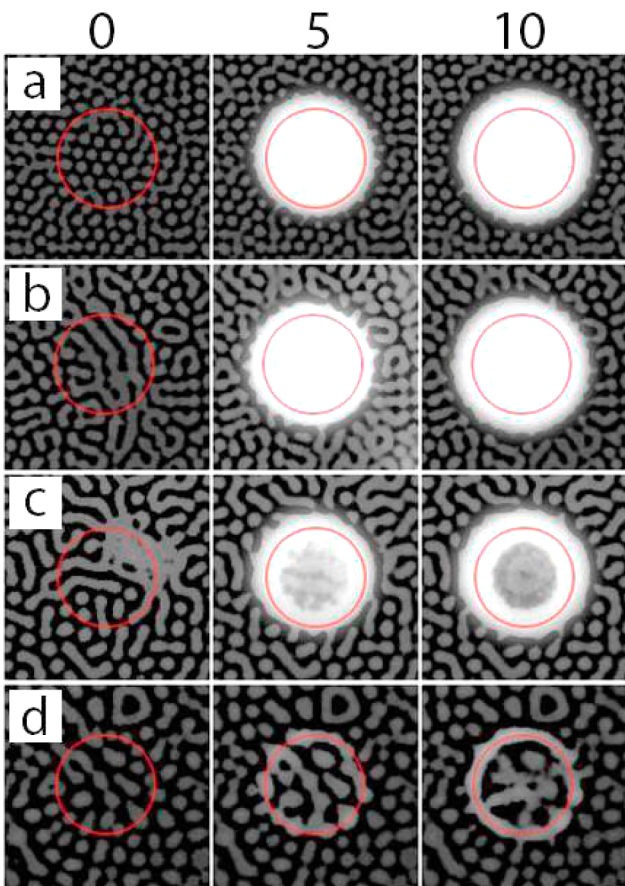


Figure 7. Pattern suppression with discs of light ($D = 2.7 \text{ mm}$, $I_{\text{disc}} = 57.3 \text{ mW cm}^{-2}$) for concentrations of ClO_2 : (a) 0.20 , (b) 0.10 , (c) 0.07 , (d) 0.05 mM . The size of the perturbation is indicated by the red circles in each frame. Each frame is $5.15 \times 5.15 \text{ mm}$. Perturbations were applied for 10 min . The first column shows patterns right before perturbation, the second is after 5 min of applying the perturbation, and the third is after 10 min of applying the perturbation (numbers above figures are in minutes). For all rows, $[\text{MA}] = 1 \text{ mM}$.

perturbation, the pattern was also suppressed in an area outside the perimeter where the perturbation was applied. This area of suppressed TP increased slightly with time (Figure 7a,b). Initially, the light consumed iodide in the area where the perturbation was applied, depleting the concentration of the dark-colored PVA-triiodide complex and giving the area a white color. Over time, free iodide ions diffused in from the edges the illuminated disc. This depleted the concentration of iodide in the region immediately surrounding the boundaries of illumination, and the area of suppression began to grow. There was no dark spot observed in the center for this range of ClO_2 concentration.

The dark spot in the middle of the illuminated area only formed when $[\text{ClO}_2] = 0.05\text{--}0.07 \text{ mM}$. With $[\text{ClO}_2] = 0.07 \text{ mM}$, after 10 min of applying the perturbation, a dark disc

surrounded by a white ring formed in the center of the perturbed region (Figure 7c). With $[\text{ClO}_2] = 0.05 \text{ mM}$, the pattern was only partially suppressed after 10 min of illumination, and a dark disc where the pattern was partially suppressed appeared in the center of the perturbed region surrounded by a white ring (Figure 7d). The dark disc in the center of the perturbed region had a higher iodide concentration than the surrounding white region, meaning that the iodide was not fully consumed by light in this area. When the concentration of ClO_2 was 0.05 mM and below, the system became much less photosensitive, and TP were not completely suppressed by light. These observations confirm that chlorine dioxide plays an important role in the photosensitivity of the CDIMA reaction.

We further investigated the role of the size of illumination on the target TP formation. Discs of illumination with diameters of $D = 1.9, 2.7$, and 4.1 mm all yielded target TP with few defects (Figure 8). Target TP formed faster the smaller the disc size. In the experiment shown in Figure 8, the target TP that formed in response to a disc of light with $D = 1.9 \text{ mm}$ (Figure 8a) was fully formed around 40 min after the initial perturbation, whereas the target TP that formed in response to a perturbation with $D = 4.1 \text{ mm}$ (Figure 8c) took almost 3 h to form. Furthermore, target TP appear to be stable for a certain period of time after formation. The target TP in Figure 8a was stable at least 50 min after its formation, looking at the pattern 40 and 90 min after the perturbation.

We observed that the larger the size of the perturbation, the larger the number of concentric rings. The smallest target TP shown in Figure 8a formed in response to illumination by a disc of light with a diameter of $D = 1.9 \text{ mm}$ and only had two rings. This target TP is the same as a unit cell of the double black eye pattern.¹⁶ The largest target TP, shown in Figure 8c, had four rings with a white spot in the center of the pattern. The number of concentric rings seen here is more than that observed in the unit cells of the black eye patterns that have been created to date. The wavelength of the target TP was always close to that of the original TP.

■ NUMERICAL SIMULATIONS AND RESULTS

We employed the Lengyel–Epstein³⁰ model with the influence of light incorporated as an additive term:¹⁴

$$\begin{aligned} \frac{\partial u}{\partial t} &= a - u - 4 \frac{uv}{1+u^2} - w(x,y) + \nabla^2 u \\ \frac{\partial v}{\partial t} &= \sigma \left[b \left(u - \frac{uv}{1+u^2} + w(x,y) \right) + d \nabla^2 v \right] \end{aligned} \quad (1)$$

Here u and v are the dimensionless concentrations of I^- and ClO_2^- ions, respectively; a , b , d , and σ are dimensionless parameters. The effect of illumination is included through the term $w(x,y)$, which is proportional to the rate of the photochemical reaction that produces ClO_2^- and consumes I^- . The fixed parameters used here are $a = 12$, $d = 1$, and $\sigma = 50$. For b in the range $0.32\text{--}0.34$, labyrinthine TP similar to those seen in our experiments are obtained.

The model equations were solved numerically by using the software package COMSOL Multiphysics 4.2a. An implicit backward differentiation formula was used for integration, and zero-flux boundary conditions were utilized along the square boundaries of the system. Random initial concentrations were chosen for one of the variables, and a stationary labyrinthine

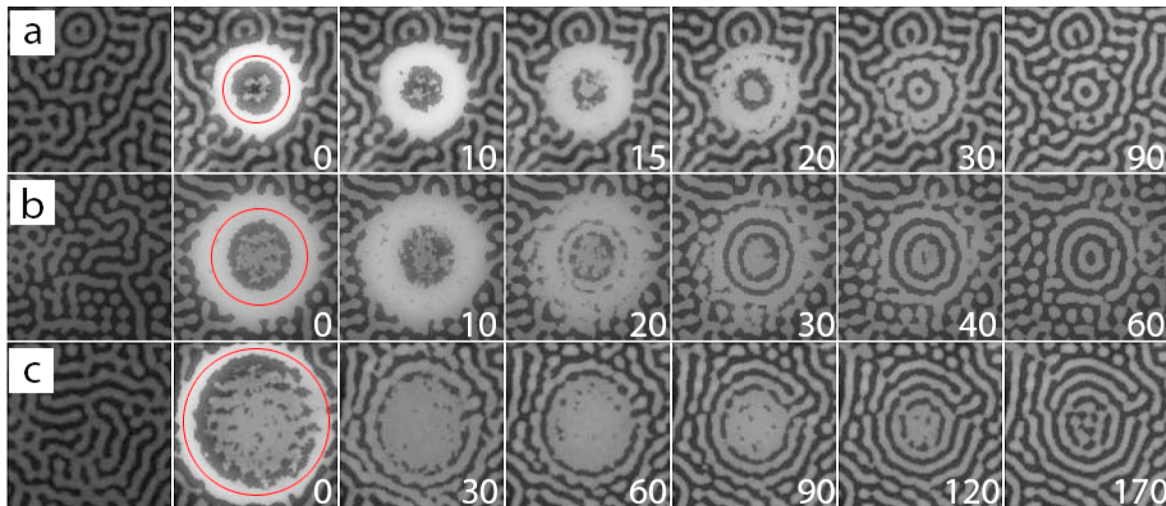


Figure 8. Effect of size of disc-shaped illumination on formation of target TP. The disc-shaped perturbations had diameters of (a) 1.9, (b) 2.7, and (c) 4.1 mm. The size of the disc is indicated by the red circles in the second column. The first column shows patterns right before perturbation, the second right after (number in the bottom right corner of each frame is the time in minutes). For all rows, $[ClO_2] = 0.07$ mM and $[MA] = 1$ mM. The initial perturbation was for 10 min. The intensity of the background illumination is $I = 5.4$ mW cm^{-2} . Frames are 4.7×4.7 mm.

pattern without illumination ($w = 0$) was used in further simulations as new initial conditions. These initial conditions correspond to the experimental snapshots labeled as “Before” perturbation.

To mimic our experiments, we set $w = 1$ inside a circular domain (Figure 9). The disc perturbation was applied for at least 100 time units (t.u.), which is long enough to suppress any pattern in the “illuminated” area. Then the perturbation was turned off ($w = 0$) and TP were allowed to recover. Figure 9 shows two examples of patterns obtained when the size of the

“illuminated” disc domain was varied. When the size of the disc perturbation is smaller ($D = 60$ space units (s.u.), Figure 9a), a target TP appears only as a transient but eventually disappears and is replaced by a labyrinthine structure. The dimensionless time units after rescaling roughly correspond to the time in seconds whereas about 100 dimensionless space units correspond to 1 cm.³¹ Further simulations revealed that when the diameter of the disc perturbation is larger than 60 s.u. then the target TP is a stationary solution of a recovered TP (Figure 9bc).

We further performed numerical simulations to study the effect of duration of illumination. Figure 10 shows snapshots of

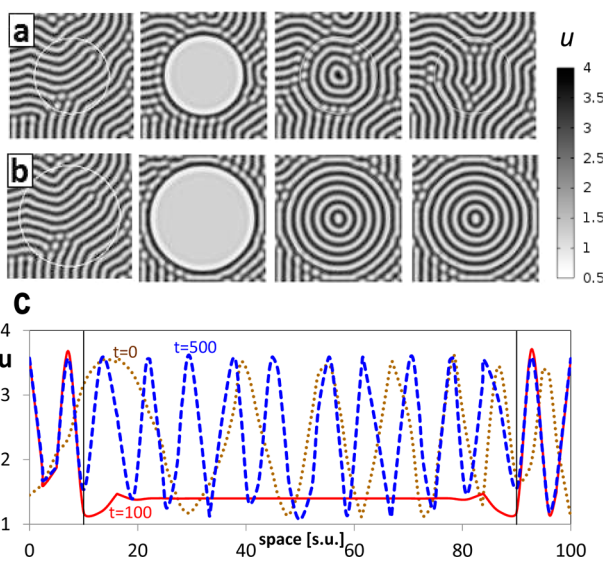


Figure 9. Target TP in the CDIMA model. Effect of size of the disc-shaped perturbation on the formation of target TP, $b = 0.32$ and $w = 1$. The disc-shaped perturbation is designated in the snapshots by the white circles; disc diameters: (a) $D = 60$ s.u.; (b) $D = 80$ s.u. The first column shows initial conditions, the second column the pattern right after 100 t.u. of perturbation, the third column after 500 t.u. of recovery, and the last column after 5000 t.u. of recovery. Frames are 100×100 s.u. (c) Profiles of dimensionless iodide concentration (u -variable) across the center of the reaction domain for the first three images shown in (b).

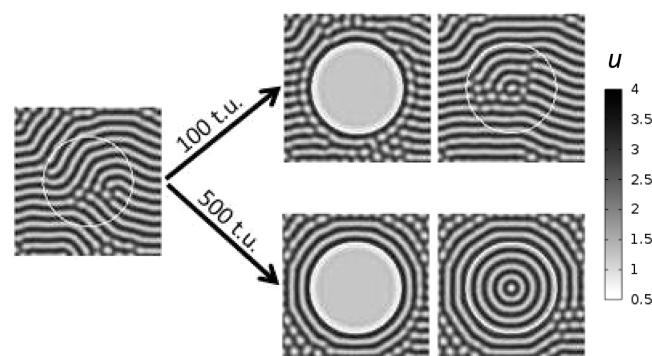


Figure 10. Effect of the duration of perturbation on the formation of target TP, $b = 0.33$ and $w = 1$. Disc diameter: $D = 60$ s.u. The snapshot on the left shows the initial conditions, the patterns after 100 and 500 t.u. of perturbation are shown in the middle, and the last column shows patterns after 5000 t.u. of recovery. Frames are 100 s.u. \times 100 s.u.

patterns that recovered after perturbations that lasted 100 and 1000 t.u. Whereas for the shorter duration of perturbation only a short-lived target TP was obtained (similar to Figure 9a, third column), the longer duration of perturbation resulted in a stationary target TP.

■ DISCUSSION AND CONCLUSIONS

Our experiments reveal that formation of target TP is favored when the concentration of chlorine dioxide and the length of the disc illumination are appropriately selected so that a dark disc with high PVA-triiodide concentration forms in the center of the perturbed area surrounded by a thick white ring. Additionally, for the chosen reactant concentrations the formation of target TP requires the presence of a certain level of background illumination during the recovery of the TP, as illustrated by Figure 5. Examining the response to one of the larger perturbations with a diameter of $D = 4.1$ mm in Figure 8c, after several minutes of recovery in background illumination the central dark spot began to lighten, meaning some of the iodide was being depleted from the region, and a thin, dark ring of higher iodide concentration formed around the lighter area in the center. This process appeared to repeat on a smaller scale until concentric rings were formed. In the case of the perturbation with $D = 1.9$ mm shown in Figure 8a, a similar mechanism seemed to occur, except that a black spot formed in the center of the target TP.

Utilizing a simple two-variable model (eq 1), our numerical simulations confirmed the formation of stable target TP for disc perturbations with diameters larger than 60 s.u., whereas for smaller discs only transient target TP were obtained, and these patterns were eventually replaced by a labyrinthine structure. The simulations also reproduced well the general trend for the effect of duration of perturbation on the formation of the target TP. The longer the duration of perturbation, the better the chance that target TP will form.

The likely explanation of these results is that the initial conditions produced by the illumination play a significant role in the formation of target TP. This formation is triggered by the pattern that forms at the boundary between the illuminated and nonilluminated regions. The illumination inside the disc domain is strong enough to suppress patterns inside that region. Meanwhile, the pattern outside the illuminated region rearranges during the illumination, taking the form of one or more concentric rings outside the boundary of illumination (Figure 10). If the concentric rings are well-developed outside the illuminated boundary, when the illumination is turned off, the target TP become stationary. However, if the concentric rings are not fully developed, then small noise and tiny heterogeneities in the gel will introduce defects in the concentric rings, and these defects will gradually lead to a random labyrinthine pattern.

The model based on the two-variable Lengyel–Epstein scheme of the CDIMA reaction gives qualitative agreement with the experimental results. However, some details of the growth dynamics are not entirely reproduced by this model. For example, the fingering mechanism and the dark spot with high iodide concentration in the center of illumination have not been obtained using this model. This is likely due to the oversimplification of the two-variable model of the CDIMA reaction. As we have shown in previous work,¹⁵ the photosensitivity of the CDIMA reaction depends on $[ClO_2]$, and this concentration becomes a variable in the presence of strong enough illumination. At low $[ClO_2]$ the system is less photosensitive, and strong illumination can result in an increase of iodide and a dark region produced in the center of illuminated region.

Target TP were also obtained in numerical simulations of a system under local feedback.³² The local feedback can change

the local and global dynamical behavior of the system and reorient Turing patterns. Our work demonstrates in both experiments and numerical simulations that target TP can be produced in an unforced system when appropriate initial conditions are created. The results of this study also support the idea that the rearrangement and reorientation of Turing patterns observed in nature can be achieved and controlled by proper spatial-temporal perturbations of the system.

■ AUTHOR INFORMATION

Present Address

[†]Division of Chemistry and Chemical Engineering, California Institute of Technology, Pasadena, CA 91125.

Notes

The authors declare no competing financial interest.

■ ACKNOWLEDGMENTS

The authors acknowledge the financial support of the U.S. National Science Foundation, grant CHE-1012428.

■ REFERENCES

- (1) Turing, A. M. A Chemical Basis of Morphogenesis. *Philos. Trans. R. Soc. London* **1952**, *237*, 37–72.
- (2) Murray, J. D. How the Leopard Gets Its Spots. *Sci. Am.* **1988**, *258* (3), 80–87.
- (3) Painter, K. J.; Maini, P. K.; Othmer, H. G. Stripe Formation in Juvenile Pomacanthus Explained by a Generalized Turing Mechanism with Chemotaxis. *Proc. Natl. Acad. Sci. U. S. A.* **1999**, *96*, 5549–5554.
- (4) Nagorcka, B. N.; Mooney. The Role of Reaction-Diffusion System in the Formation of Hair Fibres. *J. Theor. Biol.* **1982**, *98*, 575–607.
- (5) Cartwright, J. H. E. Labyrinthine Turing Pattern Formation in the Cerebral Cortex. *J. Theor. Biol.* **2002**, *217*, 97–103.
- (6) Ammelt, E.; Astrov, Y. A.; Purwins, H. G. Stripe Turing Structures in a Two-Dimensional Gas Discharge System. *Phys. Rev. E: Stat., Nonlinear, Soft Matter Phys.* **1997**, *55*, 6731–6740.
- (7) Temmyo, J.; Notzel, R.; Tamamura, T. Semiconductor Nanostructures Formed by the Turing Instability. *Appl. Phys. Lett.* **1997**, *71*, 1086–1089.
- (8) Alonso, D.; Bartumeus, F.; Catalan, J. Mutual Interference between Predators can Give Rise to Turing Spatial Patterns. *Ecology* **2002**, *83*, 28–34.
- (9) Castets, V.; Dulos, E.; Boissonade, J.; DeKepper, P. Experimental Evidence of a Sustained Turing-Type Nonequilibrium Chemical Pattern. *Phys. Rev. Lett.* **1990**, *64*, 2953–2956.
- (10) Ouyang, Q.; Swinney, H. L. Transition from a Uniform State to a Hexagonal and Striped Turing Patterns. *Nature* **1991**, *352*, 610–611.
- (11) Lengyel, I.; Kádár, S.; Epstein, I. R. Quasi-2-Dimensional Turing Patterns in an Imposed Gradient. *Phys. Rev. Lett.* **1992**, *69*, 2729–2731.
- (12) Gunaratne, G. H.; Ouyang, Q.; Swinney, H. L. Pattern Formation in the Presence of Symmetries. *Phys. Rev. E: Stat., Nonlinear, Soft Matter Phys.* **1994**, *50*, 2805–2820.
- (13) Horváth, A. K.; Dolnik, M.; Muñuzuri, A. P.; Zhabotinsky, A. M.; Epstein, I. R. Control of Turing Structures by Periodic Illumination. *Phys. Rev. Lett.* **1999**, *83*, 2950–2952.
- (14) Muñuzuri, A. P.; Dolnik, M.; Zhabotinsky, A. M.; Epstein, I. R. Control of the Chlorine Dioxide-Iodine-Malonic Acid Oscillating Reaction by Illumination. *J. Am. Chem. Soc.* **1999**, *121*, 8065–8069.
- (15) Nagao, R.; Epstein, I. R.; Dolnik, M. Forcing of Turing Patterns in the Chlorine Dioxide-Iodine-Malonic Acid Reaction with Strong Visible Light. *J. Phys. Chem. A* **2013**, *117*, 9120–9126.
- (16) Berenstein, I.; Yang, L.; Dolnik, M.; Zhabotinsky, A. M.; Epstein, I. R. Superlattice Turing Structures in a Photosensitive Reaction-Diffusion System. *Phys. Rev. Lett.* **2003**, *91*, 058302(4).

- (17) Berenstein, I.; Yang, L.; Dolnik, M.; Zhabotinsky, A. M.; Epstein, I. R. Dynamic Mechanism of Photochemical Induction of Turing Superlattices in the Chlorine Dioxide-Iodine-Malonic Acid Reaction-Diffusion System. *J. Phys. Chem. A* **2005**, *109*, 5382–5387.
- (18) Yang, L.; Dolnik, M.; Zhabotinsky, A. M.; Epstein, I. R. Turing Patterns Beyond Hexagons and Stripes. *Chaos* **2006**, *16*, 037114(9).
- (19) Berenstein, I.; Dolnik, M.; Zhabotinsky, A. M.; Epstein, I. R. Spatial Periodic Perturbation of Turing Pattern Development Using a Stripe Mask. *J. Phys. Chem. A* **2003**, *107*, 4428–4435.
- (20) Dolnik, M.; Bánsági, T., Jr.; Ansari, S.; Epstein, I. R. Locking of Turing Patterns in the Chlorine Dioxide-Iodine-Malonic Acid Reaction with One-Dimensional Spatial Periodic Forcing. *Phys. Chem. Chem. Phys.* **2011**, *13*, 12578–12583.
- (21) Feldman, D.; Nagao, R.; Bánsági, T., Jr.; Epstein, I. R.; Dolnik, M. Turing Patterns in the Chlorine Dioxide-Iodine-Malonic Acid Reaction with Square Spatial Periodic Forcing. *Phys. Chem. Chem. Phys.* **2012**, *14*, 6577–6583.
- (22) Davies, P. W.; Blanchedeau, P.; Dulos, E.; DeKepper, P. Dividing Blobs, Chemical Flowers, and Patterned Islands in a Reaction-Diffusion System. *J. Phys. Chem. A* **1998**, *102*, 8236–8244.
- (23) Míguez, D. G.; Dolnik, M.; Muñozuri, A. P.; Kramer, L. Effect of Axial Growth on Turing Pattern Formation. *Phys. Rev. Lett.* **2006**, *96*, 048304(4).
- (24) Wolff, J.; Papathanasiou, A. G.; Kevrekidis, I. G.; Rotermund, H. H.; Ertl, G. Spatiotemporal Addressing of Surface Activity. *Science* **2001**, *294*, 134–137.
- (25) Vanag, V. K.; Epstein, I. R. Localized Patterns in Reaction-Diffusion Systems. *Chaos* **2007**, *17*, 037110(11).
- (26) Vanag, V. K.; Yang, L.; Dolnik, M.; Zhabotinsky, A. M.; Epstein, I. R. Oscillatory Cluster Patterns in a Homogeneous Chemical System with Global Feedback. *Nature* **2000**, *406*, 389–391.
- (27) Zaikin, A. N.; Zhabotinsky, A. M. Concentration Wave Propagation in 2-Dimensional Liquid-Phase Self-Oscillating System. *Nature* **1970**, *225*, 535–537.
- (28) Zhou, C.; Guo, H.; Ouyang, Q. Experimental Study of the Dimensionality of the Black-Eye Patterns. *Phys. Rev. E* **2002**, *65*, 036118(5).
- (29) Brauer, G., *Handbook of Preparative Inorganic Chemistry*, 2nd ed.; Academic: New York, 1963.
- (30) Lengyel, I.; Epstein, I. R. Modeling of Turing Structures in the Chlorite Iodine Malonic acid Starch Reaction System. *Science* **1991**, *251*, 650–652.
- (31) Rudovics, B.; Barillot, E.; Davies, P. W.; Dulos, E.; Boissonade, J.; De Kepper, P. Experimental Studies and Quantitative Modeling of Turing Patterns in the (Chlorine Dioxide, Iodine, Malonic Acid) Reaction. *J. Phys. Chem. A* **1999**, *103*, 1790–1800.
- (32) Ji, L.; Li, Q. S. Effect of Local Feedback on Turing Pattern Formation. *Chem. Phys. Lett.* **2004**, *391*, 176–180.